


Jammed hard-sphere hcp crystals permeated with trivacancy tunnels F

Cite as: J. Appl. Phys. **126**, 194901 (2019); <https://doi.org/10.1063/1.5129458>

Submitted: 30 September 2019 . Accepted: 30 October 2019 . Published Online: 18 November 2019

Frank H. Stillinger , and Salvatore Torquato 

COLLECTIONS

 This paper was selected as Featured



View Online



Export Citation



CrossMark

ARTICLES YOU MAY BE INTERESTED IN

[Noncovalent force spectroscopy using wide-field optical and diamond-based magnetic imaging](#)

Journal of Applied Physics **126**, 194502 (2019); <https://doi.org/10.1063/1.5125273>

[A model of gas desorption and radiation during initial high voltage conditioning in vacuum](#)

Journal of Applied Physics **126**, 193303 (2019); <https://doi.org/10.1063/1.5124105>

[Electron-impact ionization cross sections of new SF₆ replacements: A method of combining Binary-Encounter-Bethe \(BEB\) and Deutsch-Märk \(DM\) formalism](#)

Journal of Applied Physics **126**, 193302 (2019); <https://doi.org/10.1063/1.5119087>



Lock-in Amplifiers

Zurich Instruments

Watch the Video 

Jammed hard-sphere hcp crystals permeated with trivacancy tunnels

Cite as: J. Appl. Phys. **126**, 194901 (2019); doi: [10.1063/1.5129458](https://doi.org/10.1063/1.5129458)

Submitted: 30 September 2019 · Accepted: 30 October 2019 ·

Published Online: 18 November 2019



Frank H. Stillinger¹  and Salvatore Torquato^{1,2,3,a)} 

AFFILIATIONS

¹Department of Chemistry, Princeton University, Princeton, New Jersey 08544, USA

²Department of Physics, Princeton University, Princeton, New Jersey 08544, USA

³Princeton Institute for the Science and Technology of Materials, Princeton University, Princeton, New Jersey 08544, USA and Program in Applied and Computational Mathematics, Princeton University, Princeton, New Jersey 08544, USA

^{a)}torquato@princeton.edu. URL: <http://chemlabs.princeton.edu>.

ABSTRACT

Supported by simple table-top experiments involving stackings of ball bearings and theoretical analysis, we have discovered crystal packings of identical hard spheres that are permeated by a high concentration of large tunnels and yet are jammed (mechanically stable). We show that starting with a strictly jammed hexagonal close-packed (hcp) crystal of identical hard spheres, removal of certain subsets of those spheres can produce mechanically stable vacancy arrangements involving compact (equilateral triangle) trivacancies such that they produce linear trivacancy tunnels. These tunnels can extend over the entire macroscopic length of the hcp medium, and their width is sufficient to allow contained “test” hard spheres with diameters less than $\sqrt{5} - 1 = 1.23606\dots$ to migrate over that entire length without contacting the static tunnel-wall spheres. A search for the stable (strictly jammed) periodic framework that hosts the highest density of parallel trivacancy tunnels has identified a structure exhibiting a packing fraction $\phi = \pi/\sqrt{32} = 0.55536\dots$, which is equal to 3/4 of the maximum monovalent sphere packing fraction $\phi_{\max} = \pi/\sqrt{18} = 0.74048\dots$. In that periodic arrangement, filling the interior of the contained tunnels with movable unit-diameter spheres may approach the greatest possible “rattler” density within jammed monovalent sphere systems subject to periodic boundary conditions. It will be of interest to study the physical and chemical properties of these anisotropic porous crystal structures. Our findings may have practical implications for engineered separation and catalytic processes.

Published under license by AIP Publishing. <https://doi.org/10.1063/1.5129458>

I. INTRODUCTION

The importance of packing hard particles in various types of containers and the questions that they raise have a long history, spanning problems from practical relevance to those of a fundamental nature. Bernal commented that “heaps (dense arrangements of particles) were the first things that were ever measured in the form of basketfuls of grain for the purpose of trading or the collection of taxes.”¹ On the scientific side, Kepler conjectured in 1611 that the packing fraction of identical hard (nonoverlapping) spheres, ϕ , cannot exceed that of the face-centered-cubic (fcc) arrangement and its stacking variants, such as the hexagonal close-packed crystal (hcp) ($\phi_{\max} = \pi/\sqrt{18} = 0.74048\dots$). This conjecture was proved by Hales² almost four centuries later.

“Jammed” packings are those hard-particle configurations in which each particle is in contact with its nearest neighbors in such a way that mechanical stability of a specific type is conferred to the

packing.³ Understanding the characteristics of jammed packings provides basic insights into the structure and bulk properties of crystals, glasses, granular media, colloids, random media, and biological systems.^{4–17} “Strict” jamming is the most stringent jamming category, since in such packings, there can be no “collective” particle motions that lead to unjamming, and they are stable against both uniform compression and shear deformations.³

In the case of strictly jammed packings of identical hard spheres, the focus of this work, mechanical stability requires that the average number of spheres in contact with a sphere, Z , be at least equal to 6 in the large-system limit. This minimal-contact requirement, called “isostaticity,”^{5,13} nonetheless enables packing arrangements that span a relatively wide range of packing fractions. For example, the aforementioned densest sphere packings as well as maximally random jammed configurations⁸ are strictly jammed with packing fractions $\phi = 0.74048\dots$ and $\phi \approx 0.64$, respectively.¹³

Remarkably, one can achieve strictly jammed packings of identical spheres of a unit diameter with an anomalously low density ($\phi = \sqrt{2\pi}/9 = 0.49365\dots$) that are subpackings of the densest crystal packings with a high concentration of self-avoiding “tunnels” that are chains of monovacancies permeating the structures.¹⁸ These structures are conjectured to be the strictly jammed sphere states in three dimensions with the minimal packing fraction and allow hard “test” spheres of diameter 0.73205 to freely migrate over the entire structure without contacting the static tunnel-wall spheres. Interestingly, the magnetic properties of these tunneled crystals were studied by examining the classical Heisenberg Hamiltonian for Ising, XY, and Heisenberg spins on these structures.¹⁹

Crystal structures with such controlled porous tunnels have implications for separation technology for substances whose constituent particles have just the right size to diffuse along those tunnels, leaving behind larger impurity particles.²⁰ In the event that a metallic element or alloy were to be rendered in the form of a tunneled crystal, the electronic characteristics would be strongly influenced by the structural anisotropy. The anisotropic porosities of tunneled crystals could serve as catalytic substances for reactants that fit into these pores.²¹

Therefore, a natural question of applied interest is the following: Can tunnels that are substantially wider be made in packings of identical spheres while maintaining mechanical stability? If so, can the tunnels be arranged so that they comprise a relatively large fraction of the space? This paper provides affirmative answers to both of these questions. Supported by simple table-top experiments involving stackings of ball bearings and theoretical analysis, we have discovered crystal packings of identical hard spheres that are permeated by large tunnels that are larger than a sphere diameter and yet are mechanically stable.

Section II begins with a review of the “Barlow packings,”^{22,23} the infinite family of crystalline arrangements that attain the maximum possible density for monodisperse hard-sphere systems.² Section III analyzes the geometry of compact trivacancies that can exist as isolated stable local deformations within a specific Barlow packing, the hexagonal close-packed (hcp) crystal. Section IV begins by recalling the previously studied monovacancy-tunneled Barlow packings that apparently can attain the lowest-density strictly jammed configurations of monodisperse hard spheres.¹⁸ By analogy, we then show how properly oriented compact trivacancies can be arranged relative to one another in sequential hcp layers so as to constitute a linear “trivacancy tunnel” that in principle can span an entire crystal length. The local geometrical arrangement of the static hard spheres forming the wall of such a trivacancy tunnel allows determination of intratunnel mobilities for various size-modified test spheres, with results presented in Sec. V.

The existence of the Barlow packings modified by the inclusion of periodic arrangements of monovacancy tunnels,¹⁸ in particular, as modified hcp crystals, suggests searching for trivacancy-tunneled analogs. Section VI presents an example, although evidence suggests that such analogs cannot attain the same strictly jammed low density limit apparently achieved by the monovacancy family. Finally, Sec. VII contains several discussion issues and conclusions, especially in regard to future extensions of the work reported herein.

II. BARLOW PACKINGS

For convenience in the following, it will be assumed that the monodisperse hard (nonoverlapping) spheres forming the crystal media of interest have unit diameters. If these unit-diameter spheres were to have their centers confined to a single plane (spanned by coordinates x and y), their densest arrangement in that plane would be a triangular lattice, with each sphere contacting six nearest neighbors. This periodic pattern constitutes the basic planar layer unit whose repeated replication forming similar but laterally displaced parallel layers above and below (altitude coordinate z) an initial triangular layer generates three-dimensional layered Barlow packings.

Figure 1 illustrates the primary layer packing characteristics. It explicitly shows the close-packed triangular lattice arrangement of one layer, to be designated as layer placement “A.” A subsequent parallel layer, either above or below A, has two possible lateral positions that permit its closest contact with A by resting its spheres in the available depressions presented by the A layer geometry. These two options have been located and identified, respectively, as “B” and “C” in Fig. 1. Subsequent layers will also be classified as A, B, or C depending on which of those previous arrangement types lies directly above or below in the direction z . The obvious constraint that must be obeyed to attain three-dimensional maximum sphere density is that no pair of nearest-neighbor layers has the same classifying letter. The resulting Barlow packings are then identified by their corresponding layer letter sequences, i.e.,

$$\dots \text{BACBACBCACACBCBCBCBA} \dots,$$

in which each letter cannot have its own kind as a nearest neighbor. The vertical displacement between successive (contacting) layers of unit-diameter spheres is given by

$$\Delta_z = \sqrt{2/3} = 0.81649\dots \quad (1)$$

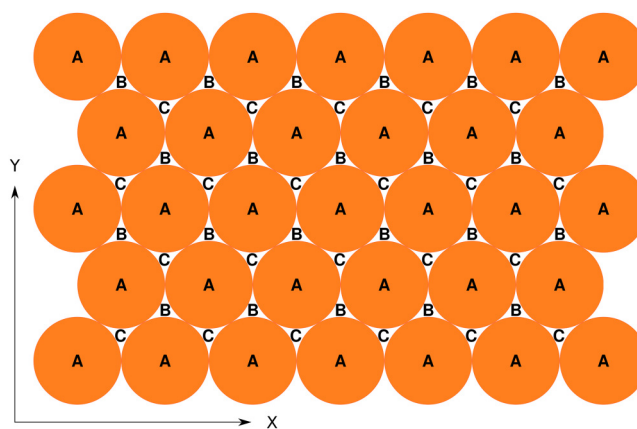


FIG. 1. Two-dimensional jammed layer “A” of unit-diameter spheres. The positions “B” and “C” identify alternate “pocket” choices for placement of neighbor layers closest to layer “A.”

Every one of the possible Barlow structures exhibits the same maximum possible unit-sphere density,² which amounts to a packing fraction given by

$$\varphi_{\max} = \frac{\pi}{\sqrt{18}} = 0.74048\dots \quad (2)$$

The structurally simplest, and best known, Barlow packings are the face-centered cubic (fcc) crystal and the hexagonal close-packed (hcp) crystal. Their respective letter sequences (aside from trivial relettering) amount to the following 3-letter and 2-letter periodic repeat units,

$$\begin{aligned} \text{fcc: } \dots \text{ABCABCABCABC} \dots &\equiv \dots (\text{ABC})_n \dots, \\ \text{hcp: } \dots \text{ABABABABABAB} \dots &\equiv \dots (\text{AB})_n \dots \end{aligned}$$

It is only the hcp crystal packings that enable one to construct the trivacancy structures described below.

III. COMPACT INTRALAYER TRIVACANCIES

The fundamental structural unit for the formation of hcp tunnels to be considered in Sec. IV is a compact equilateral-triangle trivacancy. Figure 2 illustrates the basic fact that formally, there are two distinct types of locations for an intralayer trivacancy, located between a pair of completed layers (identified as A as in Fig. 1). These alternative pocket choices are denoted by “S” and “U,” with corresponding intralayer triangle rotations that differ by 180° (equivalently 60°). Only one of these alternatives is configurationally stable (S). The other is unstable (U), lying upon a sphere in the A layer below and under a sphere in an A layer above, where either of those spheres would be unconstrained with respect to uninhibited displacement into the center of that misplaced trivacancy. Analogously, because the surrounding crystal structure is

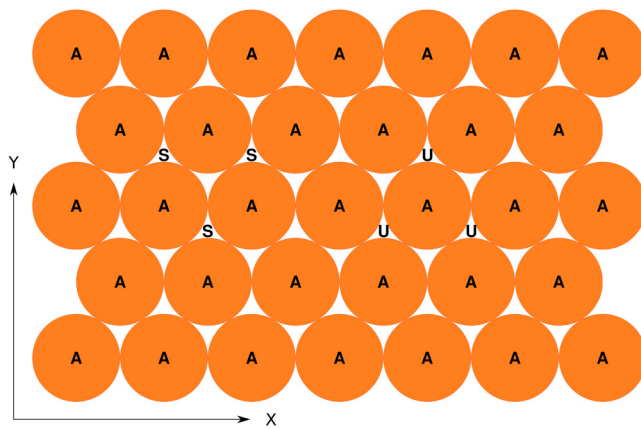


FIG. 2. Intralayer compact trivacancy locations within an hcp crystal medium, showing both the stable (S) and the unstable (U) possibilities. For consistency with Fig. 1, the complete layers below and above these location possibilities would be designated “A,” and the intermediate layer housing in either of these isolated trivacancy locations would be designated “B.”

hcp, stability (S) of an isolated trivacancy in one vertical direction implies stability in the opposite vertical direction. Note in passing that such full stability would not be possible if the surrounding crystal structure were fcc.

Each stable compact trivacancy is surrounded in its layer by nine immediate neighbors. Three of these nine contact four spheres in the layer, and the other six contact five spheres in the layer. Upon accounting as well for the hcp layers above and below that one containing the trivacancy, the contact numbers each increase by 6, to 10 and 11, respectively.

In the hcp medium, all stable compact trivacancies in B layers between A layers will exhibit the same orientation. However, stable compact trivacancies occurring in the A layers will all be rotated by 180° (equivalently 60°) compared to those in the B layers.

Single compact trivacancies can in principle also occur in the hcp medium but rotated spatially out of the *x, y* plane to reside simultaneously in two contacting layers. One of these layers would then house two of the three vacancies, and the other layer would house the remaining vacancy. Such alternative configurations play no role in the following trivacancy tunnel analysis.

It will be assumed in the following that the hcp medium of interest is subject to appropriate periodic boundary conditions that enforce the maximum possible jamming density. The presence of well isolated compact trivacancies in an hcp medium apparently does not undermine the strict jamming property of that medium.

IV. hcp VERTICAL TRIVACANCY TUNNEL

By selecting proper trivacancy positions on successive hcp layers, it is possible to create a stable trivacancy tunnel of arbitrary length. Figure 3 illustrates the relative configurations of a

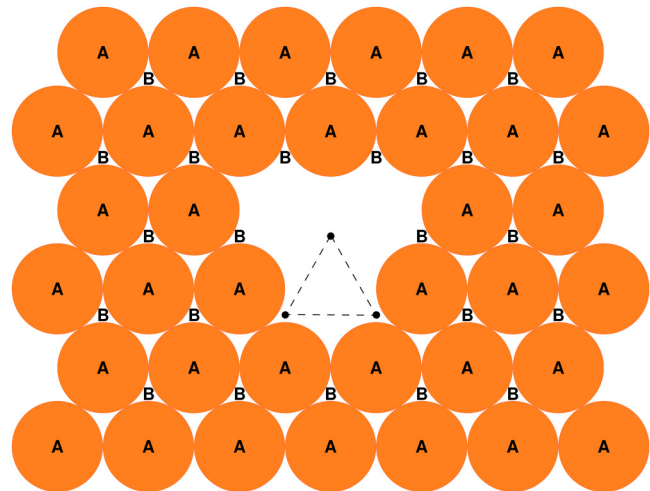


FIG. 3. Relative position of two vertically adjacent trivacancies (within nearest-neighbor hcp crystal layers). For visual simplicity, explicit sphere contours are shown only for one layer (A), while the center positions of the three missing spheres in the adjacent layer (B) are merely located by dots, connected by dashed lines.

neighboring pair of overlapping trivacancies that serve to generate a tunnel whose overall direction is parallel to the vertical z axis. The trivacancies residing on each of the A planes are replicas of one another, differing sequentially only by a z direction displacement $2\Delta_z$, from Eq. (1). The same is true of the intervening B layer trivacancies. Figure 3 clearly shows that the orientations of the overlapping A and B trivacancies differ by 180° (equivalently 60°).

Examination of Fig. 3 reveals that the centroids of each of the two trivacancy species lie, respectively, on two distinct, but closely spaced, vertical (z direction) lines. The horizontal separation between these parallel lines is $3^{-1/2}$.

It is worth mentioning that the vertical line piercing the A layer trivacancy centroids passes precisely through the center position that would have been occupied by one of the missing spheres in each of the B layer trivacancies. Of course, the reciprocal relation is also true: The vertical line piercing the B layer trivacancy centroids passes precisely through the center position that would have been occupied by one of the missing spheres in each of the A layer trivacancy centroids.

If the strictly jammed hcp crystal medium contains an even number of layers, i.e., equal numbers of alternating A and B layers, then it qualifies as required for periodic boundary conditions in the z direction. We may assume that the lateral directions also involve periodic boundary conditions. Under these circumstances, the local stacking of trivacancies in the manner indicated in Fig. 3 can be extended so as to form a trivacancy tunnel that extends the entire vertical length of the hcp crystal and crosses the periodic boundary condition without any structural disruption. That is, the tunnel can be a stable structural feature of unlimited length.

The layer geometric information illustrated in Fig. 3 permits determination of the contact numbers (from above, within, and below a chosen layer) for the spheres located at the edges of a trivacancy. These are the wall spheres of the trivacancy tunnel. One finds that for the nine trivacancy edge spheres in a single layer, two have 8 contacts, two have 9 contacts, one has 10 contacts, and four have 11 contacts. These are basic features that underlie the mechanical stability of the trivacancy tunnel contained within the jammed hcp medium. Figure 4 replicates the pattern of Fig. 3 but labels the nine trivacancy edge spheres of layer A with their respective contact numbers.

As a useful context, one can also examine the wall contact geometry for the simpler monovacancy tunnel in the hcp crystal medium. In that case, the A and B alternating layers have their respective monovacancies differing in lateral (x, y) positions by the minimum possible amount. Figure 5 presents the corresponding simpler version of Fig. 4, showing that two of the monovacancy wall spheres in layer A each have 9 contacts, while the remaining four wall spheres have 11 contacts.

The collective or strict jamming property that may apply to an hcp system penetrated by at least a single trivacancy tunnel implies that it should be feasible to construct a related mechanical model, exploiting gravity for jamming stability. Figure 6 presents a photograph of a corresponding arrangement of 336 steel ball bearings that are 11/16 in. in diameter. The example shown includes four layers of vertically stacked trivacancies resting upon a complete (no vacancy) bottom layer for stability. If more space and more ball bearings were available, there is no reason to doubt that this

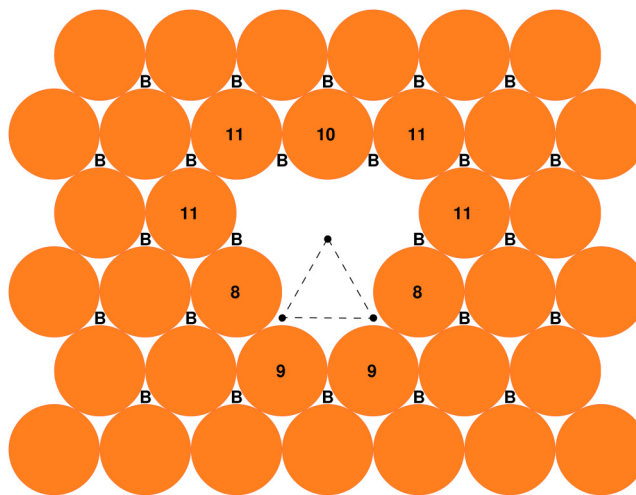


FIG. 4. Total contact numbers indicated for the A layer trivacancy edge spheres appearing explicitly in Fig. 3.

“pyramidal volcano” structure could be extended to many more layers of the vertical trivacancy tunnel.

V. INTRATUNNEL PARTICLE MOBILITY

An obvious question to be addressed about the trivacancy tunnel is how it might serve as a transport channel for a sufficiently small inserted particle. In order to understand the underlying tunnel geometry that controls such transport possibilities, it is useful to identify the location of a single central z -direction axis that passes equivalently through both A and B trivacancies in the hcp crystal medium. The obvious choice is the unique axis that lies exactly midway between the parallel pair of vertical axes described in Sec. IV that pass, respectively, through the A and B layer trivacancy centroids. This central z -direction axis will be assigned

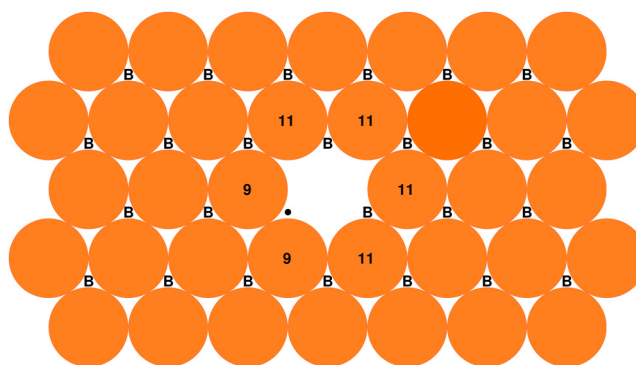


FIG. 5. Total contact numbers for the six wall spheres in layer A for a monovacancy tunnel. The center position of the single missing sphere in layer B is shown as a black dot.



FIG. 6. Photograph of a ball-bearing stacking ($N = 336$) with four layers of a single trivacancy tunnel. Each ball bearing has a diameter of $11/16$ in.

vanishing lateral coordinates,

$$x = y = 0. \tag{3}$$

In order to complete the geometric location of the x, y, z coordinate system origin, the choice for $z = 0$ will be placed midway between an A layer and its contacting B layer directly above. Referring to Eq. (1), this implies for that layer pair,

$$(z)_A = -1/\sqrt{6}, \quad (z)_B = 1/\sqrt{6}. \tag{4}$$

While moving along the tunnel-central z axis, the closest encounter to wall spheres in each A or B layer, respectively, involves just a pair of equivalent spheres. Figure 7 provides a

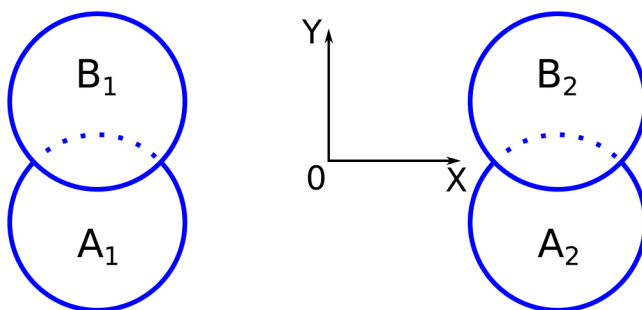


FIG. 7. Rectangular gateway for mobile (size-altered) test hard spheres, between a contacting pair of A and B layers. The coordinate origin O ($x = y = z = 0$) has been defined to occur at the midpoint of the rectangle. The four gateway-wall particles have been designated: A_1, A_2, B_1, B_2 .

TABLE I. Coordinates locating the centers of the four “gateway” spheres illustrated in Fig. 7.

Sphere	x	y	z
A_1	-1	$-1/\sqrt{12}$	$-1/\sqrt{6}$
A_2	1	$-1/\sqrt{12}$	$-1/\sqrt{6}$
B_1	-1	$1/\sqrt{12}$	$1/\sqrt{6}$
B_2	1	$1/\sqrt{12}$	$1/\sqrt{6}$

simple view from above of the locations of the corresponding four unit-diameter spheres in the contacting A and B layers just below and above the coordinate origin. The coordinates of the centers of these four “gateway” spheres have been listed in Table I. The four spheres are equidistant from the coordinate origin (indicated as \times in Fig. 7), specifically at distance

$$l_{\text{gate}} = \sqrt{5}/2 = 1.11803 \dots \tag{5}$$

If a mobile sphere were to have its center confined to the $x = y = 0$ central axis, its diameter would be subject to an upper limit to avoid colliding with the just-mentioned pairs of tunnel-wall spheres from each layer through which it passes. This limit is determined by the closest occurrence when passing precisely through the layer’s plane. From entries in Table I, one finds that the central axis at the layer height is at distance $(13/12)^{1/2}$ from the sphere centers of that layer’s wall pair. This implies that the maximum diameter of a central-axis-confined hard sphere that could move by without overlapping those fixed wall spheres is given by

$$d_{\text{max}} = \sqrt{13/3} - 1 = 1.08166 \dots \tag{6}$$

Therefore, unit diameter hard spheres could slide the entire length of the linear trivacancy-tunnel central axis without encountering any wall contact.

Unimpeded linear displacement does not identify the maximum diameter that a mobile hard sphere could possess while still being able to navigate through a trivacancy tunnel. In order to do so, however, that maximal mobile hard sphere would have to follow a nonlinear “zig-zag” path. In particular, its path would have to pass precisely through the center of each gateway rectangle (as in Fig. 7), in a direction that, at that passage moment, is perpendicular to the plane of the gateway rectangle. From Eq. (5), one sees that the maximum diameter allowing the mobile sphere to slide tangentially past the four wall spheres would be

$$d_{\text{max}} = \sqrt{5} - 1 = 1.23606 \dots \tag{7}$$

For comparison, analogous results can be computed for a vertical monovacancy tunnel in the hcp crystal. Its structure was illustrated in Fig. 5. Again, this involves a rectangular gateway of four tunnel wall unit spheres but now more closely spaced. The maximum diameter of a mobile sphere confined to move along the tunnel’s central axis turns out to be equal to

$$d_{\text{max}} = \sqrt{7/3} - 1 = 0.52752 \dots \tag{8}$$

For a movable sphere whose center is allowed to deviate from the tunnel's central axis, the corresponding maximum diameter is given by

$$d_{\max} = \sqrt{3} - 1 = 0.73205 \dots \quad (9)$$

These results obviously are substantially smaller than the trivacancy size limits (6) and (7).

VI. PERIODIC TUNNEL ARRANGEMENTS

Having determined the sphere packing geometry for a single trivacancy tunnel in Sec. IV, it is natural to inquire if a periodic arrangement of such structures could exist in the hcp crystal medium, while maintaining the overall strict jamming property. This would amount to one type of generalization of the case of monovacancy tunneled crystals.¹⁸ If such trivacancy structures can exist, they should exhibit the property of hyperuniformity.^{24,25}

Figure 8 shows a possible intralayer periodic pattern of trivacancies that might produce the desired objective. If this were an A layer, its immediate B layers below and above would involve the same trivacancy periodic pattern but rotated by 180° and translated laterally to conform to the vertical structure specified earlier in Fig. 3 for each tunnel.

Using the same steel ball bearing mechanical model packing shown earlier in Fig. 6 with a single trivacancy tunnel, we have verified the mechanical stability of three simultaneous nearest-neighbor trivacancy tunnels, arranged just as indicated in Fig. 8 as mutual nearest neighbors. Figure 9 presents such a photograph of this mechanically stable ball-bearing arrangement, demonstrating that they are at least collectively jammed³ (i.e., each sphere is locally jammed, and there are no collective motions of subsets of spheres that unjam the packing). The fact that three nearest-neighbor trivacancy tunnels are mechanically stable in this finite packing strongly suggests that one can extend the number of

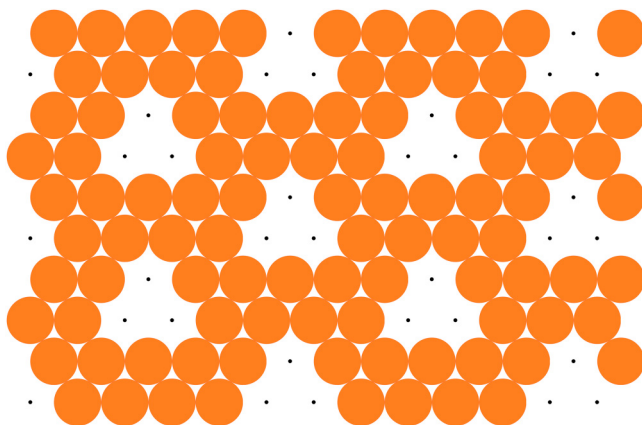


FIG. 8. Periodic intralayer pattern of trivacancies, to be used to generate a periodic array of tunnels in an hcp crystal medium. Solid black dots indicate the center positions of the vacated spheres. This pattern contains a sphere lateral density equal to three-quarters of that in the completed triangular lattice.



FIG. 9. Photograph of a mechanically stable ball-bearing arrangement in two adjacent layers of three nearest-neighbor trivacancy tunnels.

nearest-neighbor tunnels in this way with increasing system size, as desired.

If the unit vectors \mathbf{u}_x , \mathbf{u}_y , and \mathbf{u}_z are defined so as to be, respectively, aligned along the axes for the Euclidean coordinates x , y , and z that were introduced earlier, a primitive unit cell for this periodic trivacancy tunnel structure has a parallelogram prism shape and size specified by the following edge vectors:

$$\mathbf{a}_1 = 3\mathbf{u}_x - \sqrt{3}\mathbf{u}_y, \quad \mathbf{a}_2 = 3\mathbf{u}_x + \sqrt{3}\mathbf{u}_y, \quad \mathbf{a}_3 = \sqrt{8/3}\mathbf{u}_z. \quad (10)$$

This unit cell contains a basis of 18 spheres, 9 from each of a contacting pair of A and B type layers. Figures 10(a) and 10(b) indicate, respectively, how the spatial extensions of the primitive cell can be related geometrically to the short-range order of spheres and vacancies in those contacting A and B layers.

One sees in Fig. 8 that all remaining unit spheres serve as wall particles but only for the nearest trivacancy. Nearest-neighbor trivacancy pairs are separated by two lines of remaining spheres. Overall, this layer pattern involves a loss of one-fourth of the spheres compared to those comprising a complete triangular lattice layer. The corresponding trivacancy-tunneled hcp crystal, therefore, would have a packing fraction equal to

$$\varphi = (3/4)\varphi_{\max} = 0.55536 \dots \quad (11)$$

Any attempt to reduce φ by creating a periodic layer pattern with closer trivacancies evidently runs the risk of violating the strict jamming criterion.

By referring to the wall-particle contact numbers shown earlier in Fig. 4, one concludes that the average contact number per sphere, Z , in the three-dimensional periodic structure defined by

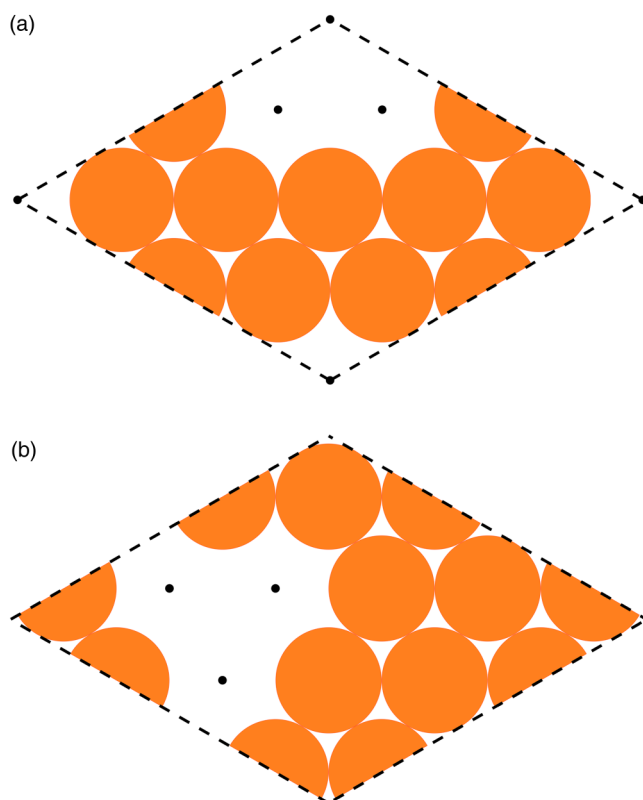


FIG. 10. Primitive cell arrangements of spheres and vacancies for the periodic trivacancy tunnel structure emerging from the layer pattern presented in Fig. 8. The inclusion patterns for A and B layers are shown, respectively, in panels (a) and (b). The boundaries of the primitive cell are shown as dashed lines. Black dots locate the positions of the centers of vacated spheres.

Fig. 8 is given by

$$\begin{aligned} Z &= (1/9)[2(8) + 2(9) + 10 + 4(11)] \\ &= \frac{88}{9} = 9.77777 \dots \end{aligned} \quad (12)$$

Thus, not surprisingly, such packings are “hyperstatic”; i.e., Z exceeds the isostatic value of 6. This result contrasts with the hyperstatic but uniform contact number per particle of 7 that is present for all remaining spheres present in hcp crystal media containing the maximum number of monovacancy tunnels.¹⁸

VII. DISCUSSION

Supported by simple table-top experiments involving stackings of ball bearings and theoretical analysis, we have discovered that a singular removal process of the hcp packing results in mechanically stable crystal packings that are permeated by a high concentration of trivacancy tunnels. In fact, one can remove up to 25% of the spheres of the original fully dense hcp crystal, yielding a packing

fraction as low as $\phi = \pi/\sqrt{32} = 0.55536 \dots$ and an average contact number per sphere of $Z = 9.77777 \dots$. These packings are at least collectively jammed, and we conjecture that they are also strictly jammed, especially since their average contact number is substantially larger than that of the strictly jammed monovalent vacancy tunnels with $Z = 7$.¹⁸ It remains for a future study to apply rigorous linear-programming jamming algorithms²⁶ to test that such tunneled crystals are truly strictly jammed.

Various stochastic methods of numerically generating jammed sphere packings typically create structures containing a low concentration of “rattlers.”^{27–29} These are particles surrounded by neighbors that are themselves jammed, but that are arranged geometrically in such a way as to form a rigid cell large enough to permit its occupant sphere to displace locally, subject to cell confinement. Based on the intratunnel sphere mobility results in Sec. V, it is worth emphasizing that trivacancy tunnels offer an extreme version of possible rattler motion. Specifically, a unit sphere inserted into a trivacancy tunnel is uninhibited for displacement along the entire (possibly macroscopic) length of the tunnel. Furthermore, a single tunnel can simultaneously host a large number of unjammed spheres that can move along its length, while experiencing collisions with one another as well as with the fixed wall spheres. These intratunnel rattlers constitute an effectively one-dimensional sphere system. It remains to be determined rigorously what the maximum possible linear density of such rattler spheres could be within a trivacancy tunnel. However, the ability of unit spheres to move unencumbered by the walls along tunnel’s central axis and to stack there in contact with each other indicates that the linear density maximum can be no less than unity.

It is reasonable to suppose that the highest density of rattlers within a three-dimensional strictly jammed surrounding framework, subject to periodic boundary conditions, would be obtained with the periodic structure identified in Fig. 8. This presumes that each of its trivacancy tunnels would be saturated internally with movable rattler spheres. If the rattler spheres within a tunnel were confined to its central axis and in mutual contact as mentioned above, the corresponding rattler density would equal the following fraction of the host framework’s sphere packing fraction,

$$(1/9)\sqrt{2/3} = 0.09072 \dots \quad (13)$$

However, this amounts to a lower bound on the maximum possible density because the rattlers can displace slightly away from that central axis, and thus away from contact with neighbor rattlers, allowing a somewhat greater intratunnel density. If indeed suitably displaced rattlers could each occupy a lateral extreme of “its own” trivacancy, the fraction in Eq. (13) would climb to the value

$$1/9 = 0.11111 \dots \quad (14)$$

This value of 11.111% rattlers considerably exceeds the roughly 1%–3% rattler density range typically observed in random jamming numerical procedures for monodisperse spheres.²⁹ It is a fascinating open question whether there exist collectively or strictly jammed packings of identical spheres whose rattler fraction exceeds 1/9.

An initial investigation of alternate strictly jammed polyvacancy tunnels hosted by an hcp crystal medium has failed to identify the possibility of larger compact vacancy clusters within a layer compared to the trivacancy case analyzed herein. It should also be mentioned for completeness that stable divacancy tunnels can be erected, but they do not present sufficient width to allow internal motion of unjammed unit-diameter rattlers.

Having established the mechanical stabilities of monovacancy and trivacancy tunnels, including their periodic crystal arrangements, it is natural to raise corresponding questions/issues about analogous divacancy tunnels. At least within an hcp unit-sphere medium, divacancies do not appear to offer any surprising structural novelties. In particular, end-to-end sequences of contacting divacancies amount structurally simply to monovacancy tunnels. Other arrangements of contacting divacancies amount to monovacancy tunnels with sidewise excess single vacancies. Of course, divacancies could be spatially placed to create monovacancy tunnel branches; however, tunnel branching goes beyond the subject matter considered here and in Ref. 18.

An interesting research issue for future study is whether our lowest-density crystal packings with trivacancy tunnels can be experimentally realized in the laboratory with colloids. It is possible that recently developed inverse statistical-mechanical techniques that enable one to design “patchy” colloid interactions for a given target structure³⁰ could offer experimentalists a guide to produce trivacancy-tunneled colloidal crystals.

ACKNOWLEDGMENTS

We are very grateful to Charles Maher for the creation of the majority of the figures and Tim Middlemas for his remarks on the manuscript. This work was supported by the National Science Foundation (NSF) under Grant No. DMR-1714722.

REFERENCES

- ¹J. D. Bernal, “The geometry of the structure of liquids,” in *Liquids: Structure, Properties, Solid Interactions*, edited by T. J. Hughel (Elsevier, New York, 1965), pp. 25–50.
- ²T. C. Hales, “A proof of the Kepler conjecture,” *Ann. Math.* **162**, 1065–1185 (2005).
- ³S. Torquato and F. H. Stillinger, “Multiplicity of generation, selection, and classification procedures for jammed hard-particle packings,” *J. Phys. Chem. B* **105**, 11849–11853 (2001).
- ⁴J. D. Bernal, “The structure of liquids,” *Proc. R. Soc. Lond. A* **280**, 299–322 (1964).
- ⁵S. F. Edwards, “The role of entropy in the specification of a powder,” in *Granular Matter*, edited by A. Mehta (Springer-Verlag, New York, 1994), pp. 121–140.
- ⁶N. W. Ashcroft and D. N. Mermin, *Solid State Physics* (Thomson Learning, Toronto, 1976).
- ⁷P. M. Chaikin and T. C. Lubensky, *Principles of Condensed Matter Physics* (Cambridge University Press, New York, 1995).
- ⁸S. Torquato, T. M. Truskett, and P. G. Debenedetti, “Is random close packing of spheres well defined?,” *Phys. Rev. Lett.* **84**, 2064–2067 (2000).
- ⁹A. Coniglio and M. Nicodemi, “The jamming transition of granular media,” *J. Phys. Condens. Matter* **12**, 6601 (2000).
- ¹⁰S. Torquato, *Random Heterogeneous Materials: Microstructure and Macroscopic Properties* (Springer-Verlag, New York, 2002).
- ¹¹C. S. O’Hern, S. A. Langer, A. J. Liu, and S. R. Nagel, “Random packings of frictionless particles,” *Phys. Rev. Lett.* **88**, 075507 (2002).
- ¹²G. Parisi and F. Zamponi, “Mean field theory of hard sphere glasses and jamming,” *Rev. Mod. Phys.* **82**, 789–845 (2010).
- ¹³S. Torquato and F. H. Stillinger, “Jammed hard-particle packings: From Kepler to Bernal and beyond,” *Rev. Mod. Phys.* **82**, 2633 (2010).
- ¹⁴Y. Jiao, F. H. Stillinger, and S. Torquato, “Nonuniversality of density and disorder of jammed sphere packings,” *J. Appl. Phys.* **109**, 013508 (2011).
- ¹⁵M. Maiti and S. Sastry, “Free volume distribution of nearly jammed hard sphere packings,” *J. Chem. Phys.* **141**, 044510 (2014).
- ¹⁶F. Giacco, L. de Arcangelis, M. P. Ciamarra, and E. Lippiello, “Rattler-induced aging dynamics in jammed granular systems,” *Soft Matter* **13**, 9132–9137 (2017).
- ¹⁷S. Torquato, “Perspective: Basic understanding of condensed phases of matter via packing models,” *J. Chem. Phys.* **149**, 020901 (2018).
- ¹⁸S. Torquato and F. H. Stillinger, “Toward the jamming threshold of sphere packings: Tunneled crystals,” *J. Appl. Phys.* **102**, 093511 (2007); *ibid.* **103**, 129902 (2008).
- ¹⁹F. J. Burnell and S. L. Sondhi, “Classical antiferromagnetism on Torquato-Stillinger packings,” *Phys. Rev. B* **78**, 024407 (2008).
- ²⁰Y. Osada and T. Nakagawa, *Membrane Science and Technology* (CRC Press, 1992).
- ²¹R. A. van Santen, *Modern Heterogeneous Catalysis: An Introduction* (John Wiley & Sons, 2017).
- ²²W. Barlow, “Probable nature of the internal symmetry of crystals,” *Nature* **29**, 186–188 (1883).
- ²³W. Barlow, “Probable nature of the internal symmetry of crystals,” *Nature* **29**, 205–207 (1883).
- ²⁴S. Torquato, “Hyperuniform states of matter,” *Phys. Rep.* **745**, 1–95 (2018).
- ²⁵T. M. Middlemas, F. H. Stillinger, and S. Torquato, “Hyperuniformity order metric of Barlow packings,” *Phys. Rev. E* **99**, 022111 (2019).
- ²⁶A. Donev, S. Torquato, F. H. Stillinger, and R. Connelly, “A linear programming algorithm to test for jamming in hard-sphere packings,” *J. Comput. Phys.* **197**, 139–166 (2004).
- ²⁷B. D. Lubachevsky and F. H. Stillinger, “Geometric properties of random disk packings,” *J. Stat. Phys.* **60**, 561–583 (1990).
- ²⁸B. D. Lubachevsky, F. H. Stillinger, and E. N. Pinson, “Disks versus spheres: Contrasting properties of random packings,” *J. Stat. Phys.* **64**, 501–524 (1991).
- ²⁹S. Atkinson, F. H. Stillinger, and S. Torquato, “Detailed characterization of rattlers in exactly isostatic, strictly jammed sphere packings,” *Phys. Rev. E* **88**, 062208 (2013).
- ³⁰D. Chen, G. Zhang, and S. Torquato, “Inverse design of colloidal crystals via optimized patchy interactions,” *J. Phys. Chem. B* **122**, 8462–8468 (2018).